CHALMERS | UNIVERSITY OF GOTHENBURG

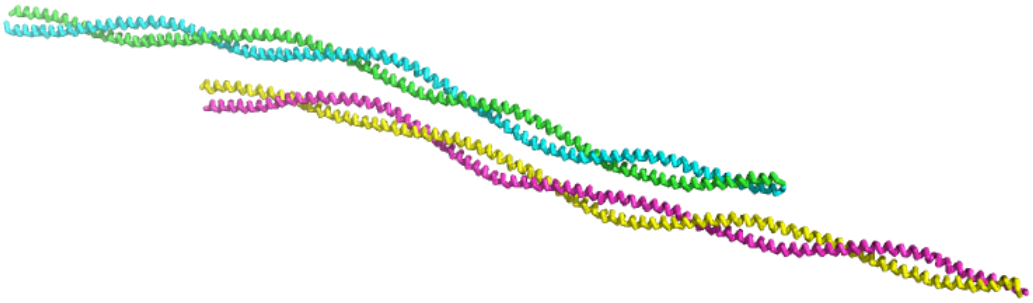

E. coli expression and purification of human β-tropomyosin

Progression towards biophysical studies of mutated sarcomeric proteins involved in congenital myopathies

Master of Science Thesis

DAVID LINDBERG

Department of Chemical and Biological Engineering
Division of Physical Chemistry
CHALMERS UNIVERSITY OF TECHNOLOGY

Institution of Biomedicine
Department of Pathology
UNIVERSITY OF GOTHENBURG

Gothenburg, Sweden, 2011

E. coli expression and purification of human β-tropomyosin

Progression towards biophysical studies of mutated sarcomeric proteins involved in congenital myopathies

DAVID LINDBERG

Department of Chemical and Biological Engineering
Division of Physical Chemistry
CHALMERS UNIVERSITY OF TECHNOLOGY

Institution of Biomedicine
Department of Pathology
UNIVERSITY OF GOTHENBURG

Gothenburg, Sweden, 2011

E. coli expression and purification of human β-tropomyosin

David Lindberg

Examiner: Bengt Nordén[1]
Supervisors: Kristina Fant[1] and Homa Tajsharghi[2]

[1]Department of Chemical and Biological Engineering
Physical Chemistry
Chalmers University of Technology
SE-412 96 Göteborg, Sweden
Telephone +46 (0)31-772 1000

[2]Sahlgrenska University Hospital
Institution of Biomedicine, Department of Pathology
Gothenburg University
SE-413 45 Göteborg, Sweden
Telephone +46 (0)31-342 1201

Cover: Sketch showing the coiled-coil structure of two dimers of human β-tropomyosin adopted from Protein Data Bank (http://www.pdb.org).

E. coli expression and purification of human β-tropomyosin

Progression towards biophysical studies of mutated sarcomeric proteins involved in congenital myopathies

Master of Science Thesis

DAVID LINDBERG

Abstract: Congenital myopathies are rare neuromuscular diseases that affect the sarcomere of human striated muscle tissue. Different congenital myopathies often present with very similar clinical features, but can often be linked to specific mutations in sarcomeric proteins such as myosin, actin or tropomyosin. This study investigates the effects of six newly discovered mutations in the gene coding for β-tropomyosin. The mutations have been linked to cap disease, nemaline myopathy and distal arthrogryposis.

Mutant and wildtype β-tropomyosin was expressed in *E. coli* using an induced batch fermentation procedure. The protein was purified to high purity by 6x-histidine tag immobilized metal affinity chromatography and succeeding gel filtration chromatography. The molecular phenotype of one mutant (E41K) was investigated by circular and linear dichroism, by which the effects on secondary structure and actin binding capacity were assessed.

Preliminary results indicate that there is no change in secondary structure between wildtype and E41K mutated β-tropomyosin. However there are indications that E41K has reduced actin binding capacity in comparison to the wildtype. These preliminary results may contribute to the molecular knowledge about β-tropomyosin, and is a step towards a better physiological understanding of these complex neuromuscular diseases.

Keywords: β-tropomyosin, actin, *E. coli*, neuromuscular disease, congenital myopathy, cap disease, nemaline myopathy, distal arthrogryposis, circular dichroism, linear dichroism.

Preface

This thesis was written by myself as the completion of my M.Sc. education at Chalmers University of Technology. I have studied the Biotechnological Engineering program for five years, where two of them have consisted of the Biotechnology master's programme with a specialization in Biomedicine. My main focus areas have been molecular biology, structural biology and biophysical chemistry, with a special interest in research concerning human physiology. I have therefore been privileged to be able to combine many of my fields of interest in this project.

The nature of this report reflects the procedure of the project. This research collaboration between Sahlgrenska University Hospital and Chalmers University of Technology on the structural and binding impacts of β-tropomyosin mutations is still very young. I have had to deal with a lot of problems that are related to start-up and project initiation. Therefore I have not been able to reach the goals that I set up during the planning of this project. It has been a rough journey with both setbacks and progress, but dealing with setbacks by means of troubleshooting and analysis is a substantial part of being a scientist. I believe that I have grown very much in this area during the length of this project, and I am most grateful to both Sahlgrenska and Chalmers for giving me the opportunity to do so.

Acknowledgements

First and foremost I would like to thank both of my supervisors for all the help, instruction and inspiration during the length of my Master's Thesis. **Homa Tajsharghi** and **Kristina Fant**, you are essential to both the completion of this report and, hopefully (knock on wood), the completing of my M.Sc degree. To the both of you, my deepest thanks.

Thanks to **Bengt Nordén** for investing the time and effort of being the examinator for this Master thesis.

Special thanks to **Louise Fornander** who helped me with fermentation procedures, **Rosmarie Friemann** for performing HPLC chromatography at Lundberg Lab and **John A. Cooper** of Washington University in S:t Louis, USA, for providing me with advice on actin polymerization. You have all contributed very much to this report, without you I would not be able to do this.

To all the others at Sahlgrenska, Gothenburg Univeristy and Chalmers who have helped me during the project; **Saba Abdul-Hussein, Karl Burman, Nils Carlsson, Catherine Kitts, Erik Lundberg, Ali-Reza Moslemi, Karin Rahl, Lili Seifi, Helene Åmand** and **all the others** that I forgot to mention. Thank you all for your kind help and advice.

To **Leif Väremo** for help and support in LaTeX during the completion of my report.

To my fellow classmates of the Biotechnology '06 class for providing a moment of rest every thursday at the Thai Basement. Evidently there is no better place to spend the better part of a lunch break.

Abbreviations

β-tm - β-tropomyosin
CD - circular dichroism
LD - linear dichroism
ATP - adenosine-5-triphosphate
ADP - adenosine-5-diphosphate
IPTG - Isopropyl β-D-1-thiogalactopyranoside
SDS-PAGE - sodium dodecyl sulfate polacrylamide gel electrophoresis
G-actin - globular actin
F-actin - filamentous actin
IMAC - immobilized metal affinity chromatography

Contents

1. Introduction

Congenital myopathies are hereditary neuromuscular diseases that can be associated with accumulations of sarcomeric proteins. These diseases are generally very rare in occurence and therefore not very well described. The sarcomere is the main contractile unit of myofibrils, the fibre structures that make up striated muscle tissue. It consists of thin and thick filaments and a number of stabilizing proteins. One component of the thin filament is tropomyosin (hereafter referred to as *tm*), an actin-binding protein which regulates muscle contraction. Recent studies conducted by Ohlsson et al. have identified several novel mutations in the β-tm gene *TPM-2* in patients suffering from various congenital myopathies.[1] The project presented in this report concerns these newly discovered mutations; E41K, K49del, G53ins, E122K, N202K and Y261C.[2, 3]

The purpose of this project is to assess the underlying mechanisms of different mutations in the β-tm gene on the structural, thermodynamic and functional properties of the protein, and to widen the knowledge about congenital myopathies. The current knowledge about congenital myopathies is in general limited to presenting clinical and morphological features and treatment is therefore limited to palliative care, i.e. medicinary measures that do not intend to cure disease, but rather handle the symptoms of the disease.[1] Understanding the functionality of the involved proteins and the molecular and physiological phenotype of the pathological mutations is imperative in understanding the mechanisms of congenital myopathies, which is an important first step in the progression towards a working treatment to these rare muscular diseases.

In this work we used circular and linear dichroism to study the effects of a number of myopathogenic mutations in human β-tm. These mutations are further described in section 2.5.. We aimed to investigate changes in β-tms secondary structure, dimerization rate and binding affinity to actin due to these above-mentioned mutations. Circular dichroism was used to determine mutation effects on protein structure such as alpha-helical content and dimer formation. Linear dichroism was used to study the binding of β-tm to actin fibers and whether this binding is affected by the mutations.

In order to study the changes in β-tm, pure samples need to be obtained of both wildtype and mutant versions of β-tm. Methods by which to achieve this were tested and developed during the initial stages of the project. Protein expression was carried out in two different expression systems; *E.coli*-based *in vitro* protein expression and *E. coli* batch fermentation. Both of these techniques were evaluated in terms of protein yield, purity and ease of expression.

2. Theoretical background

2.1. Sarcomere structure

In order to understand the nature of congenital myopathies it is important to know the basics of human muscle anatomy. Muscle tissue can be divided into two different archetypes; smooth muscle and striated muscle. Smooth muscle is the non-striated involuntary muscle tissue that exists in for example the walls of blood vessels. Striated muscle can be further divided into cardiac and skeletal muscle; cardiac muscle is the involuntary muscle tissue found in the heart, whereas skeletal muscle is the voluntary muscle tissue that is found all through-out the body, mostly connected to the skeleton and controlled by the somatic nerve system. Skeletal muscle is built up by muscle fibers, a kind of multinucleated cells formed by the fusion of precursor cells called myoblasts and surrounded by a sarcolemma membrane (Fig. 1(a)).[4] Each muscle fibre can then be further divided into sarcomeric units, which consists of an array of parallell overlapping thin and thick filaments. Each thin filament is anchored to a perpendicular protein structure known as the Z-disc, mostly made up α-actinin (Fig. 1(b)), and a single sarcomere is defined as the segment between two neighbouring Z-discs.[5] Thick filaments are mostly made up of myosin, whereas the thin filaments are built up mostly of actin and its supplementary proteins.[6] This repeating pattern of Z-discs and M-lines is what gives striated muscle tissue its characteristic appearance from where it derives its name.

2.2. Tropomyosin

Tropomyosin is a supplementary sarcomeric actin-binding protein involved in the regulation of muscle contraction. Tm is an α-helix colied-coil dimeric protein (see Fig. 2) that, when bound to actin, forms long polymers through a small binding site at each end of the individual dimers. In β-tm, as in a wide variety of proteins, a heptad repeat (a common sequence where amino acids repeat in gropus of seven) motif forms a parallell α-helical coiled-coil structure (see Fig. 3).[8] Residues at position *a* and *d* are non-polar and form a hydrophobic interface between the two strands, whereas residues *b, c, e, f* and *g* are usually polar or ionic. Residues *e* and *g* can form ionic links between the two strands and thereby add further stability to the coiled-coil structure. Residues *b, c* and *f* are located on the outside of the coiled-coil dimer and are thought to be involved in interaction with other components of the thin filament.[7] β-tm binds to the groove of the actin helix making up the thin filaments where it works in tandem with the troponin complex to start a response to increased Ca^{2+}-levels, the major signal used to initiate muscle contraction.[6] In humans, tm polymers are composed of three different isoforms of tm; α-tm, β-tm and γ-tm, which are all encoded by three different genes; *TPM1, TPM2* and *TPM3*. *TPM1* is the gene mostly expressed in fast muscle fibers such as cardiac muscle, whereas *TPM2* and *TPM3* are mainly expressed in slow type 1 muscle fibers and to some extent in fast type 2 muscle fibers and cardiac muscle. Each gene uses alternative splicing and alternative promoters to encode multiple striated muscle, smooth muscle and cytoskeletal muscle transcripts.[9]

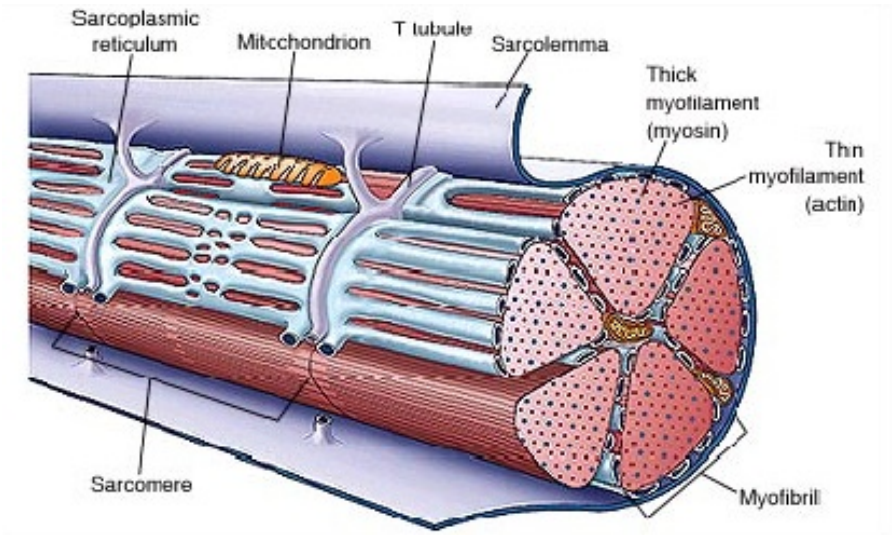

(a)

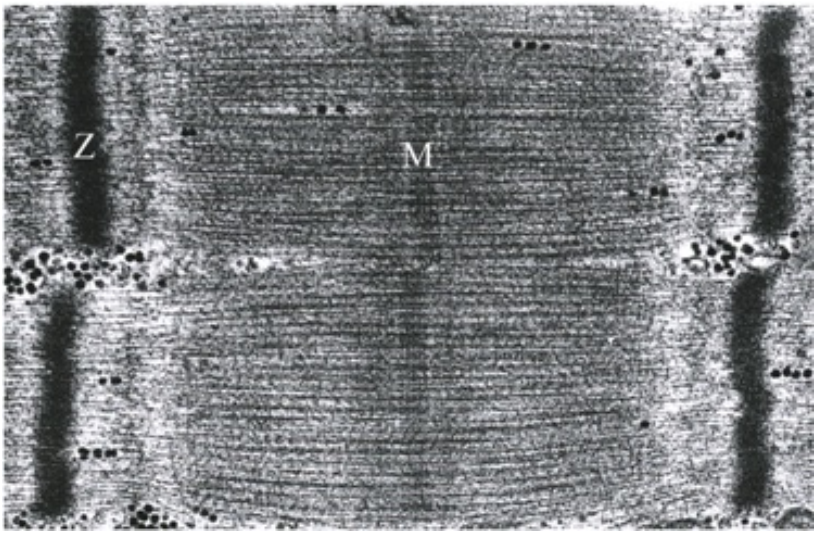

(b)

Figure 1: (a) Sketch showing the anatomy of human muscle fibers. (b) Electron microscopy image of a single human sarcomere of striated muscle tissue, visualizing the Z-disc and the M-line. (Figure adapted from ref. [7].)

2.3. Actin

Actin is the main protein making up the thin filaments of muscle fibers. It is also an important protein in cytokinesis, chemotaxis, singal transduction and other motile activities. It is among the most well-conserved proteins known in the animal kingdom, presenting very few sequence differences between such diverse species as humans and algae.[10] Actin exists in two distinct forms, globular actin (G-actin) and filamentous actin (F-actin). G-actin is the monomeric form and polymerizes into F-actin by hydrolysis of ATP in the presence of a divalent cation such as Ca^{2+} or Mg^{2+} and high salt concentrations.[11] Actin is, as mentioned above, one of the major bind-

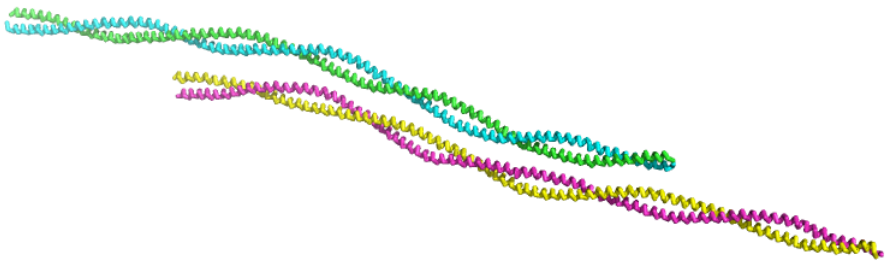

Figure 2: Crystal structure of tropomyosin, showing the coiled-coil structure of the dimer. Figure from Protein Databank (http://www.pdb.org)

ing partners of tm, which binds to the groove of the actin helix, thereby regulating muscle contraction.[11]

2.4. Congenital myopathies

Neuromuscular diseases are defined as disturbances in the motor unit, consisting of the anterior horn cell of the spinal cord, the peripheral nerve, the neuromuscular junction and the muscle fibre. It is a diverse group of diseases which mostly present similar symptoms, including hypotonia and muscle weakness. One subgroup of the neuromuscular diseases is muscle diseases or *myopathies*. Myopathies are defined as diesases where the disturbance is located in the actual muscle fibres rather than in the neuromuscular system. There exists a number of different myopathies, and they are commonly divided into inherited myopathies and acquired myopathies. Many congenital myopathies display similar clinical features and can often be linked to mutations in genes encoding for different sarcomeric proteins such as e.g. tropomyosin. The mutations that are studied in this project have been linked to several inherited congenital myopaties.[1]

Nemaline myopathy (NM) is characterized by the precense of nemaline rod structures in muscle biopsies. The clinical features include muscle weakness in the proximal, neck flexor and facial muscle along with respiratory problems. *Cap disease* is characterized by the presence of cap structures on the peripheral sarcolemma of the muscle fibers, these caps consist of disarranged accumulations of different sarcomeric proteins. The symptoms of cap disease include muscle weakness in the facial and neck muscles, hypotonia (lack of muscle tone) and respiratory problems.[9] *Congenital myopathy with type 1 fiber uniformity* is a myopathy which is characterized by the presence of type 1 fiber uniformity as the apparent morphological feature. Clinical features include muscle weakness in neck flexors and spinal muscle. *Distal arthrogryposis type 2B* (DA2B), also called Sheldon-Hall syndrome, is a subgroup of arthrogryposis multiplex congenita (AMC), a syndrome defined by the presence of mulitple joint contractures at birth. AMC in general can affect the entire body, whereas DA is confined to the distal limbs. DA2B is of one the least severe types of DA, and is together with DA1 the most common.[12]

2.5. Studied mutations

Mutations in the TPM2 gene has been shown to be present in patients suffering from a number of different congenital myopathies including cap disease, nemaline myopathy and distal arthrogryposis.[13] The mutations studied in this project have been linked to various congenital myopathies.

E41K [3], K49del [2] and N202K [2] have all been discovered in patients showing signs of cap disease, in addition E41K is also linked to nemaline myopathy. G53ins [2] and E122K [unpubl.] have been discovered in patients with Congenital myopathy with type 1 fiber uniformity, and Y261C [unpubl.] is found to be involved in distal arthrogryposis type 2B. As seen in Fig. 3 all of the mutations studied in this project are of the c, e, f or g variety located on the outside of the colied-coil dimer, as opposed to the a and d residues that make up the coiled-coil bonds. This leads to the hypothesis that the mutations major effect is on the binding of β-tm to its affiliated proteins actin and troponin.

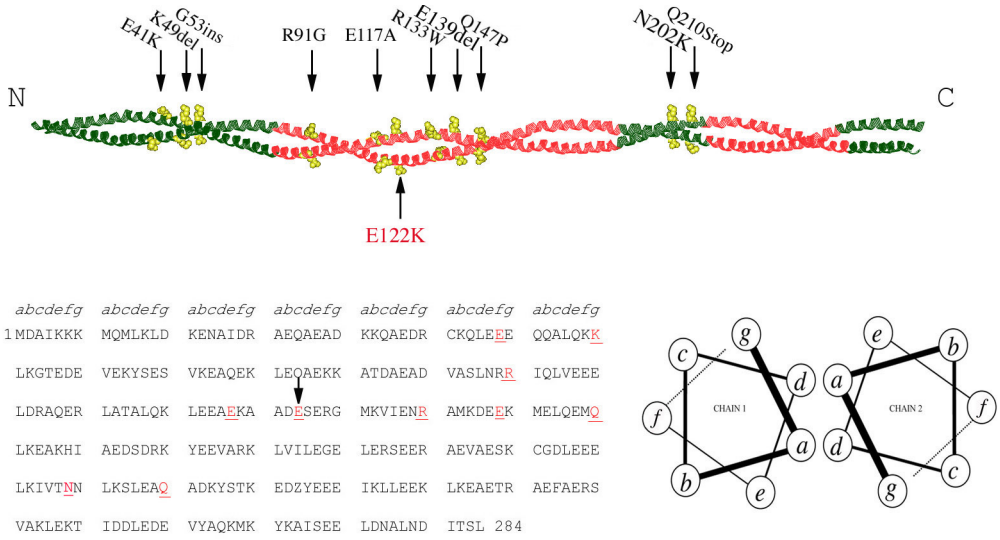

Figure 3: Top: The structure of human β-tm and the positions of the mutations investigated in this project. Bottom-left: The complete amino acid sequence of β-tm with the mutations highlighted. Alphabetic sequence on top describes the position of each amino acids place in the seven amino acid repeating pattern. Bottom-right: Sketch of the seven amino acid repeating pattern with the coil-coil interaction between residues a and d. (Figure adapted from ref. [7])

2.6. Circular dichroism

Circular dichroism is a spectroscopic method that gives information about shape and structure of *chiral molecules*, i.e. molecules whose mirror images are not superimposable. Many molecules that we find in nature are chiral, amongst them the amino acids, which means that this technique is suitable for the study of protein structure. It requires protein amounts of about 20 µg protein per sample in aqueous solution at physiological conditions, which is

more alike the native state than those used in other structural determination techniques such as crystallography or NMR. It does not, however, give the same kind of residue-specific information as either of the above-mentioned techniques.[14]

Circular dichroism is defined as the difference in the samples ability to absorb right and left polarized light (eq. 1).[15]

$$CD = A_l - A_r \tag{1}$$

In this project circular dichroism will be used to measure the α-helical content of the different tm mutants. This is in order to investigate whether the mutations introduce any structural changes that radically changes the secondary structure of the protein. The segment of the spectrum most commonly investigated for secondary structure information is 190 nm - 240 nm, as this is where CD arises in the backbone peptide bond. Conveniently, this region does not contain any CD signals from side chain residues and therefore presents a rather undisturbed CD signal from the backbone. The spectrum is distinctly defined for different kinds of secondary structures (see Fig. 4). Among the most well studied structures are α-helices and β-sheets.[15]

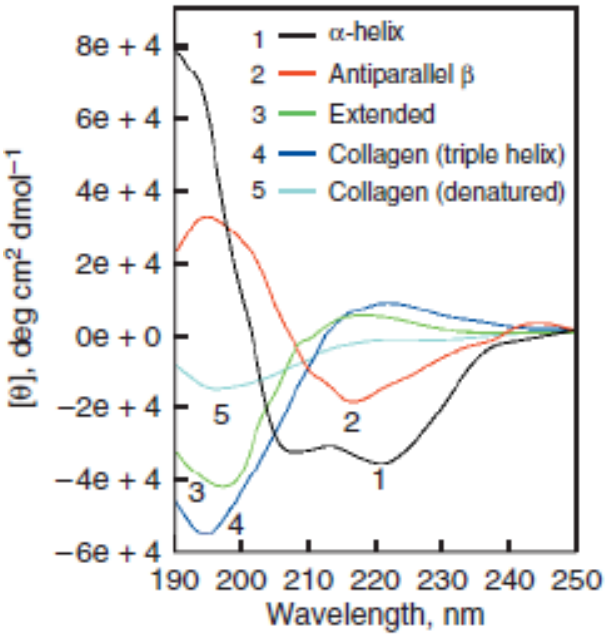

Figure 4: Graph showing the CD spectrum at 190 nm - 240 nm for various protein secondary structures. Figure adapted from ref. [14]

The α-helical structure is very common in native proteins and therefore very well studied. Its spectrum, which can be seen in Fig. 4, is characterized by a negative peak with dual localized peaks at 208 nm and 222 nm respectively. There are several CD analysis programs that are very succesful in predicting the secondary structure of a protein sample using the spectral information contained in this area.[15] β-tm is composed of 100% α-helix which means that CD is a useful tool to investigate whether any of the mutations cause a substantial change in the secondary structure.

CD can also be utilized to investigate folding dynamics.[16] This is achieved

by measuring temperature-dependent CD-spectra. The sample is heated to e.g. 90 °C, while the circular dichroism is measured at distinct temperature intervals. The resulting temperature-dependent spectrum gives a visualization of the melting temperature T_m, the refolding procedure and the reforming of protein dimers as the protein reattains its native shape with lowered temperature.

2.7. Linear dichroism

Linear dichroism is a spectroscopical method that gives information about the molecular structure of, and interactions between, macroscopically oriented molecules. Similarly to CD, LD is performed at conditions that are similar to native conditions. It is defined as the difference in absorption between parallel and perpendicularly polarized light, see eq. 2.[15]

$$LD = A_{\parallel} - A_{\perp} \tag{2}$$

In order for LD to give a useful signal, the sample must be macroscopically oriented in relation to the light beam (see Fig. 5(a)). This can be achieve, either by e.g. stretching a polymer film, or in the case of most biological molecules through the use of external force. A common example is to use LD to study interaction between small molecules and DNA, where DNA-strands can be oriented through the use of liquid shear flow. We aim to analogously investigate the binding of tm to F-actin. In the LD technique used in this study, the sample is placed in a Couette flow-cell which is described in Fig. 5(b). The sample is placed inside a glass sample holder whereafter a glass cylinder is inserted into the sample holder so as to produce a thin film of liquid along the glass wall of the sample holder. The sample holder is then rotated at high velocity while the cylinder reamins fixed, thus establishing a shear force on the liquid itself, thereby orienting the sample perpendicular to the cylinder axis.[15]

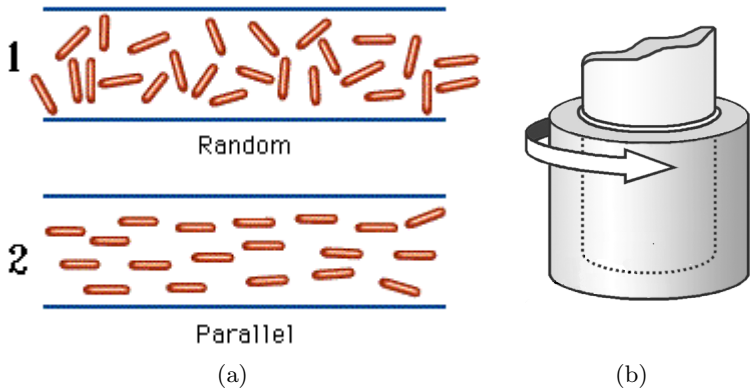

(a) (b)

Figure 5: (a) Sketch showing the difference between a randomly oriented sample (1) and a macroscopically oriented sample (2). This illustrates the macroscopic environment in the Couette flow-cell without rotational shear flow (1) and with rotational shear flow (2). (b) Sketch of a Couette-cell showing the outer sample holder rotating around the inner glass cylinder.

As described by Dafforn et al. the linear dichroism of a G-actin solution increases continuously at 205 nm when the salt concentration is rapidly increased to intiate polymerization of actin.[17] This is due to F-actin giving a distinct LD spectrum as the actin filmanets orientat due to the shear flow, whereas the monomeric G-actin molecules don't orient and therefore give no LD signal. Thus LD can be used to confirm the success of actin polymerization prior to using actin in the actin-tm binding studies. Once polymerization has been confirmed, β-tm will be added to the F-actin solution and any resulting changes in the F-actin spectrum may provide information about the actin-tm binding.

3. Materials and Methods

For detailed descriptions of the laboratory procedures, please refer to Appendix C. For detailed composition of buffers used, please refer to Appendix B.

3.1. Cloning and expression of β-tropomyosin mutants

Two different expression systems were used; in-vitro expression and batch fermentation. Both are based on *Escherichia coli* which is a gram-positive bacteria that is commonly used as a bacterial expression system in molecular biology.

3.1.1. Construction of β-tropomyosin mutants

The cDNA coding for human β-tm was cloned in a pQE-T7 (QIAGEN, Hilden, Germany) plasmid and mutated to create the mutants described in section 2.5. using the QuikChange method (Stratagene, La Jolla, US). The pQE-T7 plasmid is controlled by the T7-promotor which means that expression is induced by addition of IPTG. This is suitable for protein expression, as cells can be grown to a sizable cell mass before induction is started.

pQE-T7 contains an N-terminal 6x-Histidine tag, thus making it possible to purify the protein via immobilized metal affinity chromatography (IMAC).[18] This 6x-Histidine tag can be removed using the QIAGEN TAGZyme™ system. Prior to transfection, these vectors were amplified over night in *E.coli* DH5α and then purified using a QIAGEN Miniprep DNA purification kit.

3.1.2. *In vitro* expression

For the *E.coli*-based *in-vitro* expression, a commercially avilable expression kit was utilized, and the reaction was setup according to the provided instructions (QIAGEN, Hilden, Germany). The target protein was purified from the reaction using 6x-Histidine-tag IMAC in a small-scale magnetic bead system provided by QIAGEN. After purification, the purified samples were analyzed on SDS-PAGE and by Western blot to verify the purified protein. The SDS-PAGE analysis was performed in an Invitrogen (Carlsbad, US) X-Cell gel electrophoresis cell using Invitrogen NOVEX 10% Bis-Tris gels at 200V for 45 min. Western blot was made using an Invitrogen iBlot

blotting apparatus and anti-tm antibodies supplied by Aviva Systems Biology (San Diego, US).

3.1.3. *E.coli* batch fermentation

All SDS-PAGE gels were, unless otherwise stated, precast BIO-RAD Mini Protean TGX™Bis-Tris 10% and run in a BIO-RAD (Hercules, US) Mini Protean™electrophoresis cell at 200V, 30 min. All SDS-PAGE gels were, unless otherwise stated, stained using staining solution described in Appendix B.

The same DNA vectors were used as in the above described in-vitro expression method. The vector was transformed into *E.coli* BL21(DE3)pLysE using the calcium heat-shock method and then selected for by growth on kanamycin- and chlormaphenicol-positive agar plates. The plates were grown over night and then harvested and pooled to an inoculation culture. Four 1 L LB medium cultures were inoculated with 10 mL inoculation culture each and grown at 37 °C until OD_{600} reached 0.5. Expression was induced by addition of IPTG to 50 mg/L and the cultures were further incubated for 4 hours at 37°C. Samples of cells and culture medium were taken each hour during the induction, lysed by incubation at 95°C for 10min, purified by magnetc bead IMAC, and analyzed on SDS-PAGE to verify protein induction.

Cells were harvested by centrifugation of the culture at 5,000g for 5min. The cells were then dissolved in lysis buffer and incubated with 1 mg/mL lysozyme for 30 min on ice. The cell extract was then lysed by sonication in a VibraCell, 130W (Sonics & Materials, US). 6x-His IMAC was performed using gravity flow in a BIO-RAD disposable column loaded with 750µL QIAGEN Ni-NTA resin. The sample was loaded onto the column, washed twice with 4 mL wash buffer, and eluted in six fractions with 1mL elution buffer. All fractions collected were analyzed on SDS-PAGE to investigate the purity of the elution fractions. The elutions containing β-tm were then pooled and further purified on a HiLoad 16/60 Superdex 200 gel filtration column connected to either a Dionex (Sunnyvale, US) UltiMate 3000 or a GE Healthcare (Little Chalfont, UK) ÄKTA Explorer HPLC system. The programs used for the gel filtration is fully described in Appendix D. Apart from purifying the protein, this also dialyses the sample to remove imidazole and exchange chloride ions for fluoride ions which are less absorbant in the near-UV range. Fractions containing the majority of the β-tm peak were analyzed on SDS-PAGE and the ones corresponding to distinct gel bands were pooled and concentrated for use in spectroscopical analysis.

3.2. Polymerization of actin

In order to investigate the binding interaction between β-tm and F-actin, G-actin was polymerized by addition of KCl and $MgCl_2$ as previously described.[17, 19] To confirm the presence of F-actin, this polymerization reaction of G-actin into F-actin was studied using linear dichroism and agarose gel electrophoresis.

3.2.1. Dichroic measurements of actin polymerization

Bovine actin (Sigma) was dissolved to a concentration of 0.3 mg/mL in 50 mM PO_3^- pH 7.4. UV-Vis absorption of the actin solution was then measured from 190-350 nm in a Cary 4000™ UV-Vis spectrophotometer (Agilent Technologies, US) using a 1 mm pathlength cuvette. Circular dichroism of the actin solution was measured from 190-350 nm in a Chirascan™ instrument (Applied Photophysics, UK) using a 1 mm pathlength cuvette. Linear dichroism of the actin solution was measured in a Chirascan™ instrument, modified for linear dichroism, using a 200 µL Couette-cell with a pathlength of 700 µm. Orientational rotation was exerted at 1000 rpm. Actin was then polymerized in the Couette-cell by addition of salt to a final concentration of 50 mM KCl, 2 mM $MgCl_2$ and in some cases 0.2 mM ATP. Linear dichroism was measured at 205 or 210 nm, 1000 rpm for 1000 s in order to follow the polymerization reaction as previously described. When the polymerization reaction had finished the LD, CD and absorption spectra were measured once again as described.

After consultation from John A. Cooper of Washington University in S:t Louis, USA, the buffer used for initially dissolving the G-actin was changed from 50 mM PO_3^- pH 7.4 to G-buffer (2 mM Tris pH 8, 0.2 mM ATP, 0.5 mM DTT and 0.2 mM $CaCl_2$. Protein which was initially dissolved in 50 mM PO_3^- pH 7.4 was dialyzed against a large volume of G-buffer over 72 hours at 4 °C using 8,000 MWCO dialysis tubing. Fresh lyophilized actin was also dissolved into G-buffer. The LD and absorption spectra of the dialyzed and the newly dissolved sample were then measured again as described above.

3.2.2. Agarose gel electrophoresis of polymerized actin

An attempt to follow the polymerization of G-actin into F-actin was made using agarose gelelectrophoresis. Actin from the same source as described above was loaded on 1% agarose gels cast in G-buffer and F-buffer as previously described by Borejdo et al.[20] In addition, actin from the polymerization reaction carried out in the Couette cell was loaded on the gel individually, and along with β-tm WT and E41K (purified using IMAC only.). The gels were run for 5 hours at 4°C using an electric field strength of 2.15 V/cm^2. After 2.5 hours the running buffer (Buffer G and F) was replaced with fresh buffer in order to prevent any change in pH due to the long running time of the electrophoresis. The gels were stained with 0.125% Coomassie Brilliant Blue staining solution for 30 minutes and then destained in destaining solution over several hours.[21] The idea is that actin should migrate slower in the gel cast with F-buffer, as this should provide enough salt to cause actin to remain in the filamentous form, whereas in G-buffer, the actin is depolymerized while migrating through the gel, thereby migrating at a slower rate.

These experiments were largely inconclusive, and have not yet been repeated with the succesfully polymerized actin. Therefore, they are not described in the results section, but are rather mentioned as a point for future work.

3.3. Spectroscopic studies of β-tropomyosin mutants

Circular dichroism was measured from 350-180 nm for Wildtype and mutant β-tm in gel filtration buffer (300 mM NaF, 50 mM phosphate) using a Chirascan™ instrument and a 1 mm pathlength glass cuvette. Spectral data from 240-190 nm was used to predict secondary structure with the K2D2 algorithm.[22]

In order to study the interaction between F-actin and β-tm, linear dichroism was measured from 350-180 nm on a solution containing F-actin and β-tm. Actin dissolved in G-buffer was incubated with 50 mM KCl and 2mM $MgCl_2$ at RT, 30 min. After 30 min, 100 µL 0.1mg/mL β-tm was added to a rough actin:tm ratio of 7:1, and the solution was incubated at RT, 10 min. After incubation, linear dichroism spectra were measured using a Chirascan™ instrument modified for linear dichroism, and a 200 µL Couette flow-cell with a pathlength of 700 µm and 250 rpm rotation. It was found that the LD signal of a F-actin solution in G-Buffer diminishes over time, possibly due to protein aggregation or filament breakage. The LD-signal was therefore followed over an extended period of time to see whether addition of β-tm has any effect on the kinetics of the actin spectrum.

4. Results

4.1. *In-vitro* expression of β-tropomyosin

Initially, protein was expressed in-vitro, purified by magnetic bead IMAC and verified by Western Blot. The results are shown in Fig. 6. The blot shown in Fig. 6 lacks a band for Y261C, this is likely due to the fact that residue Y261 is in the part of the sequence which was used in immunization during antibody production. This means that a mutation in this area may very well change the antigen and therefore intervene with the antigen-antibody binding.

Problems started to arise with the in-vitro expression as the intial results could not be reproduced. Determining protein concentration using a D_C Protein Concentration Assay (BIO-RAD, Hercules, US), with BSA as a standard, confirmed this as there was no protein present in any of the elutions from the magnetic bead IMAC purification. These problems with the reproducibility of expression levels of the in-vitro expression system persisted through troubleshooting and finally caused us to abandon this expression method and instead focus on the more robust expression the protein in recombinant live *E. coli* cells. While more time-consuming, batch fermentation would give a larger amount of protein and thus be a more effective method in the long run.

4.2. *E.coli* batch fermentation

Vectors containing wildtype β-tm and E41K-β-tm were succesfully transformed into BL21(DE3)pLysE *E.coli* cells and cultured to a final pellet weight of approx. 13 g. A sample of the culture medium and of the cells was taken every hour for later analysis via SDS-PAGE to verify that the protein

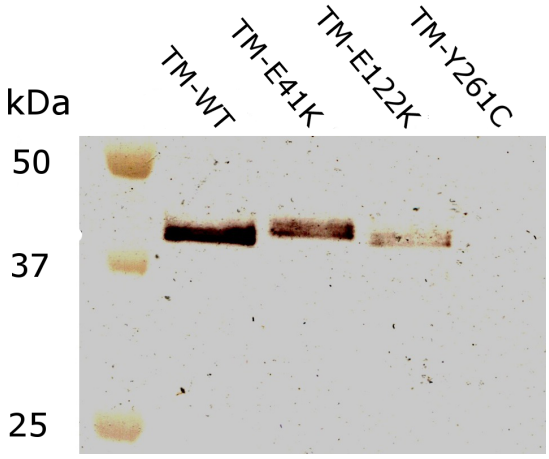

Figure 6: Western Blot of four β-tm constructs expressed using an *E. coli*-based *in vitro* expression system. β-tm was purified via magnetic bead IMAC. The β-tm band is, if present, osberved at approximately 40 kDa.

was expressed in the cytoplasm and not secreted into the medium. Cell culture samples were dissolved in 100 µL phosphate buffer pH 7.4, incubated at 95°C for 10 min, purified via magnetic bead IMAC and then loaded on an SDS-PAGE gel. The resulting SDS-PAGE can be seen in Fig. 7. At 0 hours there is no protein present, however at 1-4 hours there is a distinct band at approx. 33 kDa corresponding to β-tm, verifying that the protein is induced by the addition of IPTG. The empty lanes containing culture medium also verifies that the protein is not secreted into the culture medium at any great rate, but rather contained inside the cell.

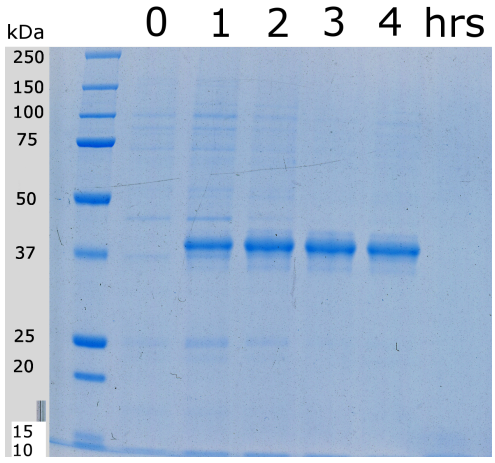

Figure 7: Induction of protein expression, verified by SDS-PAGE gel of samples taken at regular intervals after induction by IPTG. The β-tm band is, if present, osberved at approximately 40 kDa.

4.2.1. Protein purification

Protein from 1 g fermentor pellet was purified by gravity flow IMAC according to a generic protocol provided by the Ni-NTA resin manufacturer [23].

SDS-PAGE analysis shows that a large amount of contaminant proteins are present in the elution fractions (see Fig. 8(a)). This led to optimization of the IMAC purification protocol by decreasing the amount of Ni-NTA resin used to pack the column and increasing the concentration of imidazole in the wash buffer. [23] Optimization of the IMAC protocol greatly reduced the amount of contaminant proteins as can be seen in Fig. 8.

The gel filtration chromatography purification conducted on our in-house Dionex HPLC system were unsuccessful, with no apparent peaks in the range where we expected the protein to elute. Two peaks appeared later at 240 minutes (120 mL). These peaks were analyzed by UV-Vis spectrometry and were found to be imidazole from the elution buffer.

The entire gel filtration step was instead attempted at the Lundberg Lab of Gothenburg University and their ÄKTA Explorer HPLC system. Using the same column matrix, but a smaller column size, we were able to separate β-tm from the contaminants present in the IMAC elutes. The spectrum from the gel filtration can be seen in Fig. 9. The first high peak represents β-tm and the other peaks are contaminant proteins and other molecules present in the buffer of the loaded sample. SDS-PAGE confirmed the molecular weight of the first peak to approx. 40 kDa (see Fig. 10). The small bands present at about 70 kDa are likely β-tm dimers.

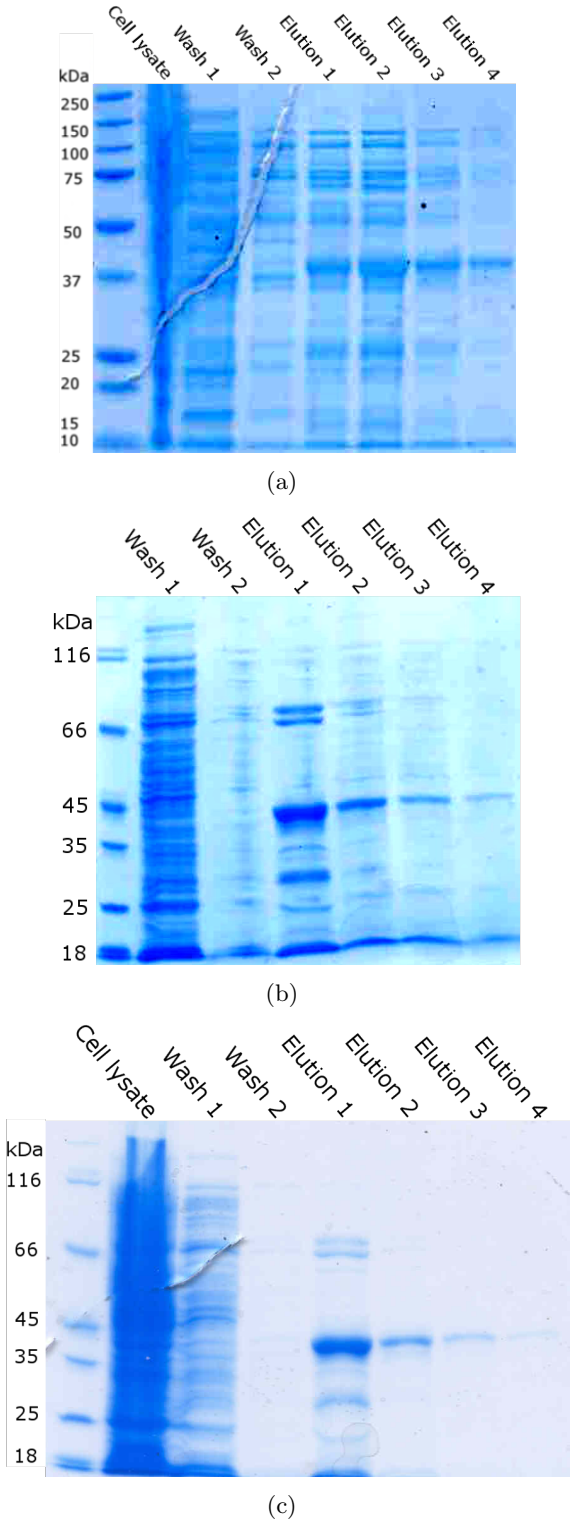

Figure 8: (a): SDS-PAGE gel loaded with the different fractions collected during 6x-Histag IMAC prior to optimization. β-tm band visible at approximately 40 kDa. (b), (c): SDS-PAGE gels loaded with the different fractions collected during 6x-Histag IMAC of (b) Wild-type β-tm and (c) E41K β-tm. β-tm band visible at approximately 40 kDa.

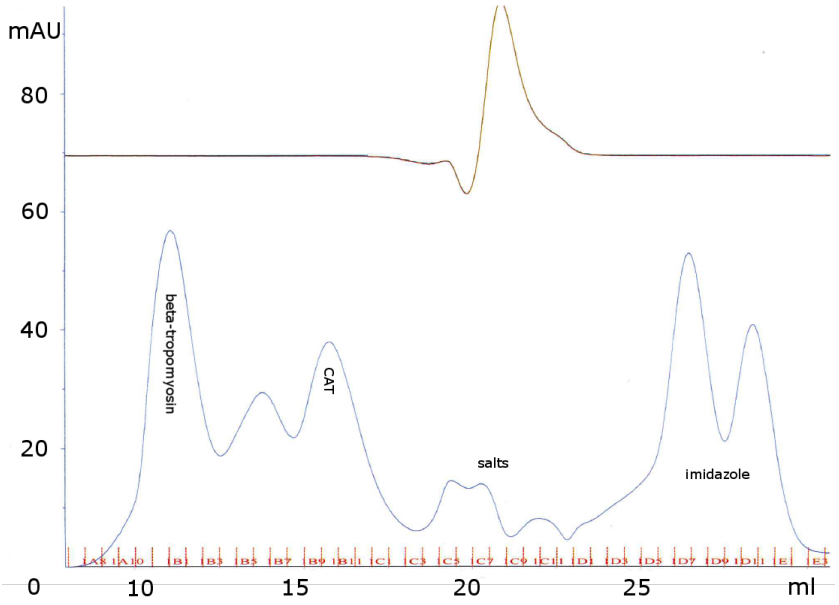

Figure 9: Absorption spectrum showing the absorbance at 280 nm (blue) and conductivity (brown) of the fractions collected during gel filtration chromatography.

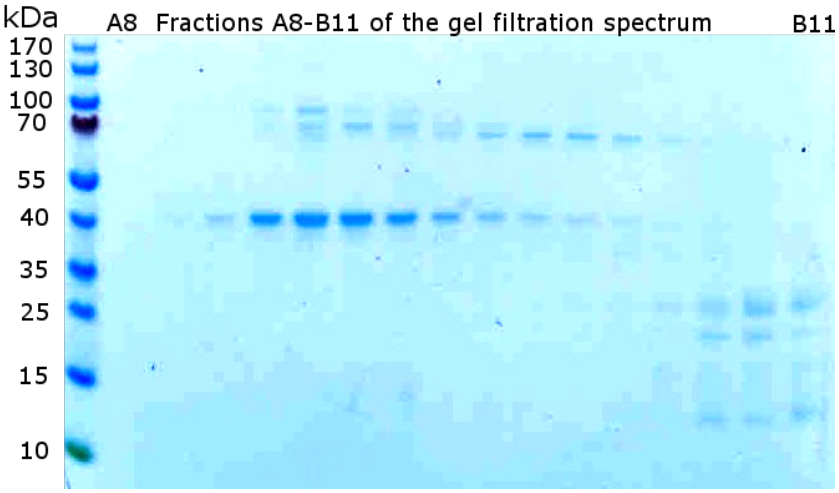

Figure 10: SDS-PAGE gel loaded with the different fractions collected during Gel filtration chromatography. The β-tm band is visible at approximately 40 kDa. The band visible at appr. 30 kDa is possibly CAT (chloramphenicol acetyl transferase).

4.3. Actin polymerization

Actin in phosphate buffer

G-actin was dissolved in phosphate buffer, polymerized and analyzed using circular and linear dichroism, the resulting graphs are shown in Fig. 11. The G-actin CD spectrum has a distinctly negative signal between 240-200 nm which is consistent with the spectrum provided by Dafforn et al. for F-actin.[17] Upon addition of salt this negative signal disappears almost completely and the spectrum is mostly noise. The LD spectrum of G-actin has two positive peaks between 240-200 nm indicating that the system has some orientation that gives rise to the signal. This signal is consistent with that Dafforn et al. presents for F-actin [17], albeit with a considerably lower signal strength despite using higher concentration of actin. Upon addition of salt solution this signal is decreased to a level that makes it inseparable from the instrument noise, indicating that the actin does not polymerize as expected.

We hypothesized the necessity of ATP in the polymerization of G-actin into F-actin, therefore, the polymerization reaction was initialized with 0.2mM ATP in addition to the salt solution. The resulting LD spectrum from this extra ATP was similar if not identical to the spectrum without ATP (Fig. 11), leading to the conclusion that extra ATP is not necessary to produce the effect seen in the LD spectrum.

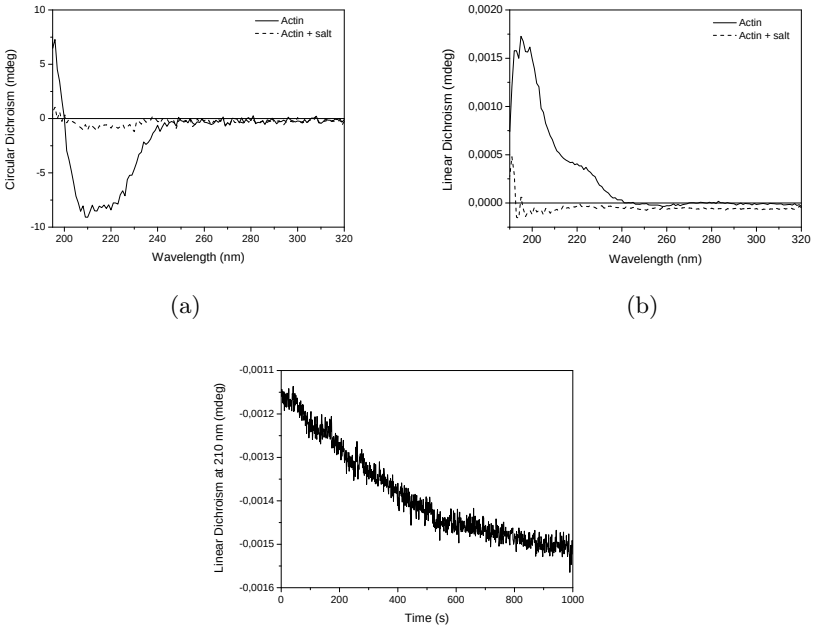

Figure 11: Initial results for spectroscopic studies of actin, polymerized in phosphate buffer. (a) CD spectrum of actin before and after addition of 50 mM KCl and 2 mM $MgCl_2$. (b) LD spectrum before and after addition of 50 mM KCl and 2 mM $MgCl_2$. (c) Plot showing the change in LD signal at 210 nm over time after the addition of 50 mM KCl and 2 mM $MgCl_2$. Evidently, the polymerization was unsuccessful.

Actin in G-buffer

Following the advice of John A. Cooper of Washington University, S:t Louis, USA (see 3.2.1.) dichroic measurements were redone using G-actin initially dissolved in phosphate buffer, that had been dialysed into G-buffer (see appendix B). The resulting LD and absorption spectra can be seen in Fig. 12. In contrast to the above-mentioned measurements made in phosphate buffer, the samples in G-buffer showed no distinct signal either pre or post salt addition. The conclusion drawn from this was that dissolving the lyophilized actin in phosphate buffer irreversibly damages the G-actin so that it cannot be polymerized. Instead we opted to dissolve fresh lyophilized actin in G-buffer.

New LD measurements were made on actin that was dissolved directly into G-buffer. The reuslting spectra can be seen in Fig. 13. Dissolving actin directly into G-buffer provided a solution to the problem of polymerizing actin. There is a distinct LD signal from F-actin after KCl and $MgCl_2$ were added, proving that the sample contains polymerized actin. Further, the kinetic linear dichroism measured at 205 nm after salt addition at time 0 s show that the F-actin is unstable when exposed to the shear flow of the couette flow-cell. The dichroism from F-actin reaches a maximum at around 700 s and then slowly diminishes. This effect would prove useful

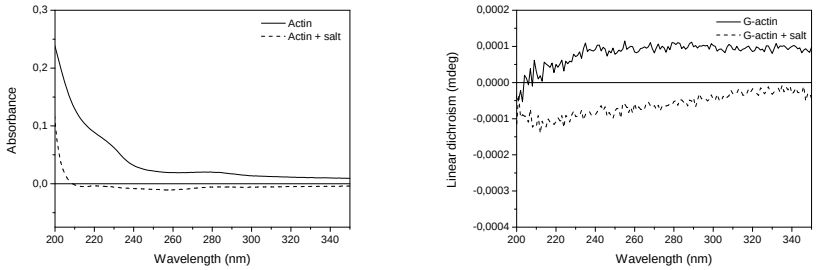

(a) (b)

Figure 12: Troubleshooting the polymerization process of actin. Actin dissolved in phosphate buffer was dialyzed against G-buffer prior to the polymerization. (a) Absorption spectrum of actin before and after addition of 50 mM KCl and 2 mM $MgCl_2$. (b) LD spectrum of actin before and after addition of 50 mM KCl and 2 mM $MgCl_2$. The dialysis removed all traces of F-actin but did not improve the polymerization.

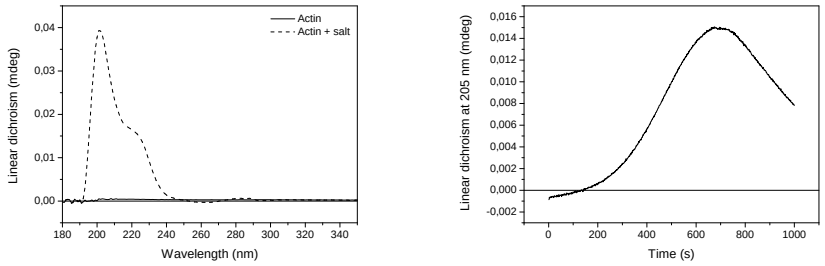

(a) (b)

Figure 13: Successful actin polymerization, performed in G-buffer. (a) LD spectrum of an actin solution before and after addition of 50 mM KCl and 2 mM $MgCl_2$. (b) Time-dependent LD measured at 205 nm after salt addition at time 0 s.

when studying the effects of β-tm on F-actin (see section 4.4.).

4.4. Spectroscopic studies of β-tropomyosin mutants

Once pure protein samples had been obtained, CD-spectra were measured for β-tm wildtype and mutant E41K in 300 mM NaF and 50 mM phosphate. Due to slight concentration differences in the two samples, the CD-spectra were normalized against the concentration of each sample. This eliminates any differences due to protein concentration and shows that the shapes of the two spectra are nearly identical. There is a clear α-helical structure pattern in the spectrum with dual local negative peaks at 208 and 222 nm. Predicting the secondary structures from the spectrum using the K2D2 prediction tool [22] (here non-normalized data was used) gives roughly 90% α-helix and 0% β-sheet for both constructs, further confirming that there was no observed difference in secondary structure between the wildtype and the mutant E41K.

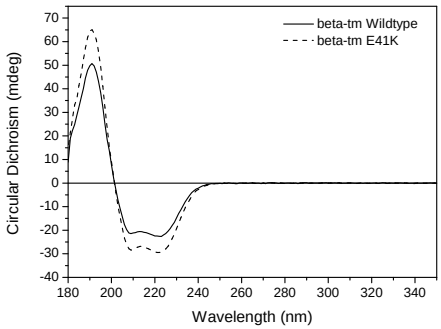

Figure 14: Normalized CD-spectra of β-tm wildtype and mutant E41K in gel filtration buffer (300 mM NaF, 50 mM phosphate).

Linear dichroism was measured a solution containing F-actin and β-tm. Resulting spectra are shown in Fig. 15 The results from the kinetic LD measurements, shown in Fig. 15(b), indicate that the LD of a pure F-actin solution diminishes over time. If wildtype β-tm is added to the solution, the LD of the solution does not diminish over time, but rather, increases somewhat. This indicates that β-tm has some kind of stabilizing effect on actin filaments, which may be due to binding. Addition of E41K β-tm provides some stability, but not as much as wildtype β-tm. As a control, GF-buffer without any protein was added to the solution providing similar stability as E41K β-tm.

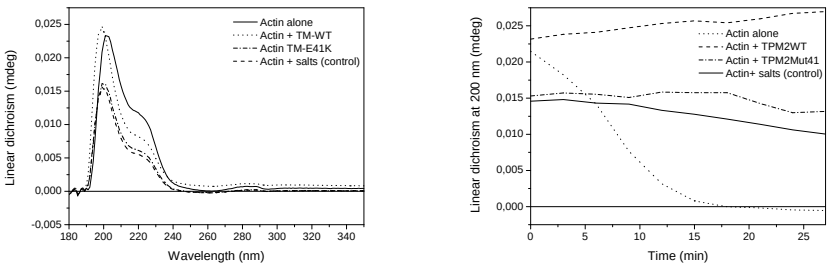

(a) (b)

Figure 15: (a): LD spectra measured for F-actin; without β-tm, with wildtype β-tm, with E41K β-tm, and with addition of GF-buffer without β-tm as control. (b): LD-signal at 200 nm measured over time for F-actin; without β-tm, with wildtype β-tm, with E41K β-tm, and with addition of GF-buffer without β-tm as control.

5. Discussion

In vitro expression vs. batch fermentation

In vitro expression is a desirable method to use when small quantities of protein is required, and a fully equipped life science laboratory is not available. However, as proven by the studies conducted in this project, it is not a very robust method. Protein expression appears to be highly unreliable despite the use of a commercial expression kit. It is also, unless the expression kits are made in-house, a very expensive method as the entire kit has to be obtained commercially. In comparison, batch fermentation provides a much more reliable robust expression. However it is more time-consuming and laboratory-intensive, and requires a well-equipped life science lab. In this project we opted for the use of batch cultivation as we opted for the high amount of protein and the greater robustness of the expression system.

Migration pattern of β-tm on SDS-PAGE

It is worth to note that on the various SDS-PAGE gels that are presented in this report, β-tm appears to have a migration pattern more similar to that of a protein with a molecular weight of approximately 40 kDa, instead of its native 33 kDa. The 6x-histidine tag along with the short linker adds on approximately 1 kDa of molecular weight, however this does not explain the large discrepancy between migration behaviour and acutal molecular weight. It is, however, reported by Crowe et al. that adding or replacing amino acids can shift protein bands, suggesting a molecular weight several kDa higher than expected, thus explaining the somewhat slower migration of β-tm in our gels.[18] A possible way to confirm the molecular weight of the purified protein is to analyze it by mass spectroscopy, thus verifying both the molecular weight and the amino acid sequence.

Despite the optimization of the 6x-histidine tag IMAC purification there still exists some contaminants in the elutions. The most dominant are the single band at approximately 30 kDa, and the double band at approximately 65 kDa. The single band at 30 kDa could possibly be CAT (chloramphenicol-O-acetyl transferase) which is a protein conferring chloramphenicol resistance in *E. coli*.[24] The strain we are using (BL21 (DE3) pLysE) is resistant to chloramphenicol which makes this a likely candidate for the 30 kDa contaminant. CAT is 25 kDa in actualy size but has been reported to migrate on SDS-PAGE as an apparent 30 kDa-sized protein. As the functional native state of β-tm is in dimer form, one possible solution to the band visible at 65 kDa is that it represents the dimerized form of β-tm. Despite the reducing and denaturing environment of an SDS-PAGE it is still common to see di- or polymerized forms of proteins in gels. With β-tm monomers being 33 kDa it seems plausible that dimers would migrate at an apparent size of around 65 kDa.

Upscaling of purification

The resulting gels and chromatography spectra shown in this report are from purifications based on 1 g of *E. coli* pellet. In order to purify the

entire pellet from one fermentation of *E. coli* (approx. 14 g) the purification protocol needs to be scaled up to fit the larger amount of cells. Upscaling of protocols is usually not as trivial as merely scaling all parameters but usually requires further optimization. Parameters such as Ni-NTA resin volume, imidazole concentraiton in the various buffers used and the amount of buffer used to elute the protein may need to be optimized.

Issues with concentrating the purified protein

β-tm is, as seen on the cover image, a highly linear protein that doesn't form the globular structure that is common to most proteins. This makes it behave rather differently in certain situations. For example, one problem during the length of the project was choosing correct MWCO filters for concentrating samples. The proper MWCO limit for linear proteins is 6-10 times lower than the actual molecular weight of the protein. Initially, with β-tm being approximately 33 kDA we opted to used a 10k MWCO filter, which yielded very poor reuslts. At times the protein would disappear entirely during concentration. Better results were achieved when the 10K MWCO membrane was exchanged for a 3K MWCO membrane. Also, it is important to be sure that protein has not adhered to the membrane by thoroughly pipetting up and down when retrieving the protein from the concentration tube.

Precipitation by means of 'salting out' is one alternative way of concentrating the sample. Salting out stabilizes the structure of the protein and is therefore well-suited for concentrating samples that are to be used in structural studies.[25]

Actin polymerization

The dichroic measurements of the actin polymerization intially produced spectra that were distinctly different compared to the results presented by Dafforn et al.[17] When comparing the spectra from our experiments with the CD and LD spectrums presented by Dafforn et al. our data for G-actin was consistent with ttheir reuslt for F-actin. As the signals were generally lower in our data, a suggested solution to this contradiction was that our data originated from trace amounts of F-actin in the G-actin sample. This is consistent with the F-actin-like signal disappearing when the sample was dialysed to G-buffer instead of phosphate buffer. When the polymerization reaction was followed using LD at 210 nm the signal was decreasing over time. This is possibly due to any trace amounts of F-actin being broken into monomeric G-actin and brought out of solution through precipitation. This is not in line with the data shown by Dafforn and therefore suggested that there was some issue with the polymerization protocol we are following.

After consultation from John A. Cooper, the buffer used to dissolve the lyophilized actin was changed from 50 mM phosphate into G-buffer by dialysis. Following this exchange of buffer the distinct differences between pre- and post-salt addition spectra disappeared. This discrepancy was attributed to the presence of trace amounts of F-actin in the actin solution. It appears that these traces have disappeared as a result of the change in buffer, which indicates that the G-buffer succesfully converts any F-actin into G-actin.

However, no apparent polymerization of actin could be observed. Possibly, the initial dissolving the actin into phosphate buffer is the problem.

New lyophilized actin was dissolved into G-buffer instead of phosphate buffer. Additionally, the solution was left stirring at 4°C over night. This seems to have produced a different starting material compared to the actin solution dissolved in phosphate buffer. The new solution polymerized very well into F-actin, giving similar signals as those presented by Dafforn et al.[17] We can therefore conclude that in order to achieve satisfactory polymerization of G-actin into F-actin, the lyophilized actin pellet should be dissolved into G-buffer in 4°C over a prolonged period of time.

Mutant effects on secondary structure

As visualized in the spectrum shown in section 4.4. there is no distinct difference in the shape of the normalized CD spectrum exhibited by wildtype and E41K β-tm. Moreover, the K2D2 prediction confirms this analysis as it predicts at least 90% α-helix for both proteins. It should be noted that the K2D2 prediction was not able to predict a 100% α-helix as is expected, however, there was no significant difference between the two samples, and 0% β-sheet, which we interpret as an indicator that they are of identical secondary structure.

Actin binding potential of *E. coli*-produced β-tm

LD measurements presented in section 4.4. indicate that wildtype β-tm produced in *E. coli* does have actin binding potential. These results show that our expression system works with the method we are using to study actin-binding potential.

The results show that there is a significant difference in actin binding capacity between wildtype and E41K β-tm. The E41K mutation is in f position which, as indicated in section 2.5., is one of the positions proposed to be involved in interaction with other proteins. It should be mentioned that these results are still preliminary and further experiments need to be made to definitely confirm this difference in actin binding capacity.

6. Future work

This project will continue beyond this report. As of the writing of this report, wildtype and E41K β-tm has been expressed and purified to approximately 0.15 mg protein per g cell pellet. This, while not a fantastic yield, is more than enough for spectroscopic studies, meaning that the current purification protocol can be used in the future to purify the remaining six mutants. It would add further strength to the purification if the protein could be western blotted to absolutely confirm that the purified protein is in fact β-tm.

Both wildtype and E41K β-tm have been analyzed for changes in secondary structure and actin-binding potential, leading to an indication that there is no major change in secondary structure, but a slight difference in actin-binding. It still remains to investigate their dimerization and fold-

ing dynamics via temperature-dependent circular dichroism. We also aim to further confirm the difference in actin-binding potential by using other techniques to study protein interaction, e.g. isothermal titration calorimetry and agarose gel electrophoresis of F-actin.

The remaining six mutants have been produced to *E. coli* fermentor pellet but still remain to be purified and analyzed in the same manner as E41K. Given that the first important method development has already been done, it should not be as time-consuming to do this for the rest of the mutants.

References

[1] Monica Ohlsson. *Muscle diseases with damaged sarcomeres - causes and consequences*. PhD thesis.

[2] M. Ohlsson, S. Quijano-Roy, N. Darin, G. Brochier, E. Lacene, D. Avila-Smirnow, M. Fardeau, A. Oldfors, and H. Tajsharghi. New morphologic and genetic findings in cap disease associated with {beta}-tropomyosin (TPM2) mutations. *Neurology*, 71(23):1896, 2008.

[3] H. Tajsharghi, M. Ohlsson, C. Lindberg, and A. Oldfors. Congenital myopathy with nemaline rods and cap structures caused by a mutation in the beta-tropomyosin gene (TPM2). *Archives of neurology*, 64(9):1334, 2007.

[4] Gerard Tortora. *Essentials of Anatomy and Physiology*. John Wiley and Sons Ltd, Chichester, 2009.

[5] P. Young, C. Ferguson, S. Bañuelos, and M. Gautel. Molecular structure of the sarcomeric z-disk: two types of titin interactions lead to an asymmetrical sorting of α-actinin. *The EMBO journal*, 17(6):1614–1624, 1998.

[6] Bruce Alberts. *Molecular Biology of the Cell*. Garland Science, New York, 2002.

[7] Homa Tajsharghi. *Mysoin myopathy - A new disease entity*. PhD thesis.

[8] H. Tajsharghi. Unpublished review article.

[9] M. Ohlsson. Muscle diseases with damaged sarcomeres-causes and consequences. 2011.

[10] M.F. Carlier. Actin polymerization and ATP hydrolysis. *Advances in Biophysics*, 26:51–73, 1990.

[11] AM Gordon, E. Homsher, and M. Regnier. Regulation of contraction in striated muscle. *Physiological reviews*, 80(2):853, 2000.

[12] M. Bamshad, L.B. Jorde, and J.C. Carey. A revised and extended classification of the distal arthrogryposes. *American Journal of Medical Genetics Part A*, 65(4):277–281, 1996.

[13] V.L. Lehtokari, C. Ceuterick-de Groote, P. de Jonghe, M. Marttila, N.G. Laing, K. Pelin, and C. Wallgren-Pettersson. Cap disease caused by heterozygous deletion of the [beta]-tropomyosin gene tpm2. *Neuromuscular Disorders*, 17(6):433–442, 2007.

[14] N.J. Greenfield. Using circular dichroism spectra to estimate protein secondary structure. *Nature protocols*, 1(6):2876–2890, 2007.

[15] A. Rodger and B. Norden. *Circular Dichroism and Linear Dichroism*. Oxford University Press, Oxford Oxfordshire, 1997.

[16] N.J. Greenfield. Using circular dichroism collected as a function of temperature to determine the thermodynamics of protein unfolding and binding interactions. *Nature protocols*, 1(6):2527–2535, 2006.

[17] T.R. Dafforn, J. Rajendra, D.J. Halsall, L.C. Serpell, and A. Rodger. Protein fiber linear dichroism for structure determination and kinetics in a low-volume, low-wavelength couette flow cell. *Biophysical journal*, 86(1):404–410, 2004.

[18] J. Crowe, B.S. Masone, and J. Ribbe. One-step purification of recombinant proteins with the 6xhis tag and ni-nta resin. *Molecular biotechnology*, 4(3):247–258, 1995.

[19] T. Kim, J.A. Cooper, and D. Sept. The interaction of capping protein with the barbed end of the actin filament. *Journal of molecular biology*, 2010.

[20] J. Borejdo and H. Ortega. Electrophoresis and orientation of F-actin in agarose gels. *Biophysical journal*, 56(2):285–293, 1989.

[21] R. Kim, H. Yokota, and S.H. Kim. Electrophoresis of proteins and protein-protein complexes in a native agarose gel. *Analytical Biochemistry*, 282(LBNL–45795), 2000.

[22] C. Perez-Iratxeta and M.A. Andrade-Navarro. K 2 d 2: Estimation of protein secondary structure from circular dichroism spectra. *BMC structural biology*, 8(1):25, 2008.

[23] QIAGEN. *The QIAexpressionist*. Valencia, CA, 2003.

[24] V.M. Bolanos-Garcia and O.R. Davies. Structural analysis and classification of native proteins from e. coli commonly co-purified by immobilised metal affinity chromatography. *Biochimica et Biophysica Acta (BBA)-General Subjects*, 1760(9):1304–1313, 2006.

[25] David Whitford. *Proteins*. John Wiley & Sons, Chichester, 2005.

Appendices

Appendix A: Sequence of wildtype human TPM2

Amino acid sequence of wildtype human TPM2, mutated amino acids are underlined in the sequence. For a complete description of mutations, please refer to section 2.5..

```
        10         20         30         40         50         60
MDAIKKKMQM LKLDKENAID RAEQAEADKK QAEDRCKQLE EEQQALQKKL KGTEDEVEKY

        70         80         90        100        110        120
SESVKEAQEK LEQAEKKATD AEADVASLNR RIQLVEEELD RAQERLATAL QKLEEAEKAA

       130        140        150        160        170        180
DEESERGMKVI ENRAMKDEEK MELQEMQLKE AKHIAEDSDR KYEEVARKLV ILEGELERSE

       190        200        210        220        230        240
ERAEVAESKC GDLEEELKIV TNNLKSLEAQ ADKYSTKEDK YEEEIKLLEE KLKEAETRAE

       250        260        270        280
FAERSVAKLE KTIDDLEDEV YAQKMKYKAI SEELDNALND ITSL
```

Appendix B: Solutions and Buffers

Lysis Buffer

- 50 mM NaH_2PO_4
- 300 mM NaCl
- 10 mM imidazole

Wash Buffer

- 50 mM NaH_2PO_4
- 300 mM NaCl
- 40 mM imidazole

Elution Buffer

- 50 mM NaH_2PO_4
- 300 mM NaCl
- 250 mM imidazole

Gel filtration Buffer

- 50 mM NaH_2PO_4
- 300 mM NaF

G-Buffer 10x

- 20 mM Tris
- 2 mM ATP
- 5 mM DTT
- 2 mM $CaCl_2$
- pH adjusted to 8 with HCl

To make F-Buffer; add 20 mM $MgCl_2$ to G-buffer 10x.

Agarose gelelectrophoresis sample buffer

- G-buffer
- 20% glycerol
- 0.2% BFB

Tris-Glycine running buffer 5x

- 125 mM Tris
- 1.25 M Glycine
- 50 mL 10% SDS
- fill to 1 L with H_2O

SDS-PAGE sample buffer, 4x

- 2.5 mL 1 M Tris-HCl pH 6.8
- 0.8 g SDS
- 4 mL glycerol
- 400 µLBromophenol Blue (BFB)
- 2 mL 14 M β-mercaptoethanol
- 1.1 mL mQ-H_2O

Coomassie staining solution

- 0.5 g Coomassie Brilliant Blue
- 20 mL acetic acid
- 100 mL methanol
- 80 mL mQ-H_2O

Destaining solution

- 75 mL acetic acid
- 50 mL methanol
- 875 mL mQ-H_2O

Appendix C: Protocols

Expression of β-tm in *E.coli* batch fermentation

1. Thaw one tube of log-phase BL21(DE3) pLysE and inoculate 3 ml LB/cam (25 µg/ml).
2. Culture at 37°C, 200 rpm, until OD600 reaches 0,5-1,0 (2-3h).
3. Divide the culture into 2 eppendorf tubes, 1,5 ml each, and prepare competent cells according to the $CaCl_2$-method:
   (a) Harvest the cells by cfg 5000 rpm, 5 min.
   (b) Discard the supernatant. Resuspend the cells in 750 µL50 mM $CaCl_2$.
   (c) Incubate on ice, 5 min.
   (d) Cfg 5000 rpm, 5 min.
   (e) Discard the supernatant. Resuspend the cells in 100 µL50 mM $CaCl_2$.
   (f) Incubate on ice at least 20 min.
4. Transform the cells with your desired plasmid:
   (a) Add 500ng plasmid DNA to the cells; incubate on ice, 20 min.
   (b) Heat chock at 42°C (heat block), 2 min.
   (c) Incubate on ice, 5 min.
   (d) Add 1 ml LB-medium and transfer to culture tubes.
   (e) Culture at 37°C, 200 rpm, 1 h.
5. Add 500 µLLB/amp(150 µg/ml) (leading to a final conc of amp 50 µg/ml); culture for 2 h more, 37°C, 200 rpm.
6. Transfer the cultures to eppendorf tubes, cfg 4500 rpm, 5 min.
7. Remove almost all of the supernatant; resuspend the cells in the remaining medium.
8. Spread on 4 plates, LB/amp (50 µg/ml) + cam (25 µg/ml); incubate at 37°C over night.
9. Scrape the bacteria off the plates in 2 x 5 ml LB/plate, using the spreader.
10. Pool the bacterial suspensions and adjust volume to 40 ml.

11. Inoculate 4 x 1 L LB/amp (50 µg/ml), each with 10 ml of the suspension.

12. Check OD600 at start; culture at 37°C (laboratory room temperature), 200 rpm until OD600 reaches 0,3-0,6 (approximately 5 hours).

13. Take out a 1,5 ml sample before induction, cfg 8000 rpm, 5 min; store at -20°C. Induce protein expression with 50 mg/l IPTG (prepare a 25 mg/ml solution in water to be used the same day), for approximately 4-5 h. Take a sample for SDS-PAGE every hour to follow the expression.

6x-His IMAC purification of β-tropomyosin

1. Thaw 1 g E.coli pellet and resuspend in 5 mL Lysis Buffer. The solution will be rather filamentous.

2. Add lysozyme to 1 mg/mL. Incubate solution on ice for 30 min.

3. Sonicate the sample at 50% amplitude, 6x10s pulses and 10s pause time. Repeat if the solution is still filamentous/viscous.

4. Centrifuge the solution at 10,000g for 30 min to remove cellular debris. In case of no 15-mL Falcon-rotor, divide the sample into eppendorf tubes and then pool the fractions.

5. Filtrate the supernatant through a 0.45µmsyringe filter.

6. Fill a BIO-RAD Poly-Prep Chromatography column with 750µLQiagen Ni-NTA resin. Equillibrate the column with 3 column volumes of mQ-water.

7. Cap the column and resuspend the resin in 500µLmQ-water.

8. Transfer the resin to a 15 mL Falcon tube and mix with the filtrated clear cell lysate. Incubate with shaking at 4C, 30min.

9. Pour the solution back into the column and collect the flowthrough in a 15 mL Falcon tube.

10. Wash the column with 2x4mL Wash Buffer. Collect flowthrough in 15 mL Falcon tubes.

11. Eluate with 6x1mL Elution buffer. Collect the flowthrough in eppendorf tubes.

12. Cap the column and wash the resin with 4 column volumes of 0.5M NaOH for 30min. Collect flowthrough in a 15 mL Falcon tube.

13. Store the column in 30% EtOH at 4C. Wrap all openings in parafilm.

Appendix D: Program used for gel filtration HPLC

```
Pressure.LowerLimit =  0 [bar]
Pressure.UpperLimit =  10 [bar]
MaximumFlowRampDown =  Infinite
MaximumFlowRampUp =  Infinite
%A.Equate =  "S300"
%B.Equate =  "%B"
%C.Equate =  "Etanool"
%D.Equate =  "%D"
Pump_Pressure.Step =  0.01 [s]
Pump_Pressure.Average =  Off
Sampler.PumpDevice =  "Pump"
Data_Collection_Rate =  2.5 [Hz]
TimeConstant =  0.60 [s]
UV_VIS_1.Wavelength =  280 [nm]



 0.000 Autozero
Flow =  0.500 [ml/min]
%B =  0.0 [%]
%C =  0.0 [%]
%D =  0.0 [%]
InjectValve.Inject
Pump_Pressure.AcqOn
CollectFractions =  No
UV_VIS_1.AcqOn
Flow =  0.500 [ml/min]
%B =  0.0 [%]
%C =  0.0 [%]
%D =  0.0 [%]


350.000 Flow =  0.500 [ml/min]
%B =  0.0 [%]
%C =  0.0 [%]
%D =  0.0 [%]
Flow =  0.010 [ml/min]
%B =  0.0 [%]
%C =  100.0 [%]
%D =  0.0 [%]

1500.000 Flow =  0.010 [ml/min]
%B =  0.0 [%]
%C =  100.0 [%]
%D =  0.0 [%]
UV_VIS_1.AcqOff
Pump_Pressure.AcqOff

End
```